Droplet Formation Mechanism in Microfluidical Devices

Mechanismus der Tröpfchenbildung in mikrofluidischen Geräten

Emil Grigorov*

*Technical University of Sofia, Faculty of German Engineering and Economics Education,
e-mail: egrigorov@FDIBA.tu-sofia.bg

Abstract — The work presents a numerical study of the parameters influencing the droplet formation in a flow-focusing microfluidic device. The idea is to give an explanation for the mechanisms behind the emulsion formation in those type of systems. The utilized numerical method, volume-of-fluid (VOF) is validated against the results from an experimental study from the literature. After the validation was completed, the influence of the continuous phase velocity was studied in detail, revealing that with increasing value for u_c, droplet length reaches a point of saturation. The Ca number is introduced as a measure for the acting forces on the dispersed phase. The results revealed that for increasing capillary numbers Ca, above a value around 0,01 droplet size decreases noticeably and a transition from the dripping towards the jetting regime of droplet formation occurs.

Zusammenfassung — In der Arbeit wird eine numerische Studie der Parameter vorgestellt, die die Tröpfchenbildung in einer mikrofluidischen Vorrichtung beeinflussen. Die Idee ist, eine Erklärung der Mechanismen hinter der Emulsionsbildung in dieser Art von Systemen zu geben. Die eingesetzte numerische Methode, Volume-of-Fluid (VOF), wird mit den Ergebnissen einer experimentellen Studie aus der Literatur validiert. Nach der Validierung wurde der Einfluss der Geschwindigkeit der kontinuierlichen Phase im Detail untersucht, wobei sich zeigte, dass mit steigendem Wert für u_c die Tröpfchenlänge einen Sättigungspunkt erreicht. Die Ca-Zahl wird als Maß für die auf die dispergierte Phase wirkenden Kräfte eingeführt. Die Ergebnisse zeigen, dass mit zunehmender Kapillarzahl Ca oberhalb eines Wertes von $0,01$ die Tröpfchengröße deutlich abnimmt und ein Übergang vom Tropf- zum Strahlregime der Tröpfchenbildung stattfindet.

I. Introduction

In recent years, microfluidic devices have emerged as a novel tool for the realization of different biological and medical processes. The decreased reagents volumes, usually in the micro/nanoliters range, can significantly reduce reaction times and energy consumption for a certain process [1]. Droplet-based microfluidics, which encapsulates different chemical or biological compounds into individual picolitre-droplets, allows the isolation of reactions from their surroundings, protecting them from unwanted mixing and allowing better control over a massive number of independent reactions. These small microreactors have provided an easily implementable and relatively cheap approach for a broad range of processes including cell lysis [2], DNA purification [3], polymerase chain reaction (PCR) [4] and many more. Therefore, understanding the mechanisms behind the droplet generation is crucial for the efficiency of a droplet-based microfluidic systems. Droplets formation usually occurs when two immiscible liquids intersect each other. The process is achieved by passive (using pressure-driven flow and the channel geometry) methods. The specific design of the microfluidic channels makes it possible for an aqueous phase, usually water, to be sheared by another continuous phase (hydrocarbon oils, fluorocarbon oils etc. [5]) and produce uniform-sized drops. Different geometry designs are possible, the most utilized in the praxis are: T-junction [6-7], flow-focusing [8-9], or co-flowing [10]. Figure 1 shows the flow-focusing device as an example.

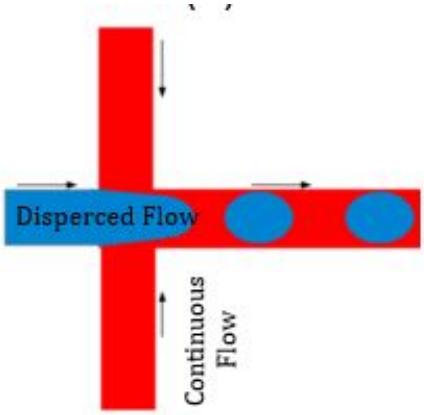

Fig. 1. Flow-focusing microfluidical setup for the droplet generation.

For the design of microfluidic devices operating in droplet flow regime, prior knowledge of droplet size, shape, formation frequency or pressure drop are essential. A good way to collect in advance this information for a new setup is by utilizing a predictive CFD (Computational Fluid Dynamics) model and interpreting the influences of some fluid

properties on the droplet breakup. Few numerical studies on droplet-based microfluidics were carried out in the past years utilizing different numerical techniques (for example level set (LS) [11] or Lattice Boltzmann method (LBM) [12-13]). All these techniques show the usefulness of CFD methods as a valuable predictive tool. In this article we investigate numerically the droplet formation in a flow-focusing microfluidic channel by utilizing the volume of fluid (VOF) method. After a validation of the model, we make a parameter study on the effect of the continuous phase velocity. The droplet formation is investigated and analyzed by means of the capillary number Ca.

II. Mathematical model, geometrical setup and boundary conditions

In the present study three-dimensional simulations of droplet formation in a flow-focusing geometry are carried out utillizing a finite volume method based CFD solver from ANSYS Fluent 16. The two immiscible fluids, water and oil as well as their interface, are modelled by the Volume of fluid (VOF) method. In this method, following the Eulerian principle, the fluid flow is treated as a continuum. A phase fraction parameter, α, is used to indicate the presence of each phase at every location of the domain. Fluid properties such as viscosity and density are smoothed and the surface tension force is distributed near the interface as a body force in the Navier-Stokes equations. With this, the system of coupled partial differential equation consists of the continuity equation (1) the momentum balance equation (2), and the phase fraction equation for α (3) becomes [14]:

$$\frac{\partial \rho}{\partial t} + \nabla \cdot \rho U = 0 \tag{1}$$

$$\frac{\partial (\rho U)}{\partial t} + \nabla \cdot (\rho U U) = -\nabla p + \nabla \cdot (\mu [\nabla U + \nabla U^T]) + F_s \tag{2}$$

$$\frac{\partial \rho \alpha}{\partial t} + \nabla \cdot \rho \alpha U = 0 \tag{3}$$

In the equations above, U is the velocity vector field, p is the pressure field and μ the viscosity of the fluid. F_s represents the surface tension force

Only one such transport equation (3) needs to be solved since the volume fraction of the other phase can be inferred from the constraint:

$$\alpha_c + \alpha_d = 1 \tag{4}$$

where the index 'c' stands for continuous and 'd' for dispersed phase. The continuous phase (water) is introduced through the two side channels and the dispersed phase (oil: octane +2,5 % SPAN 80) is entered from the main (central) channel. The information about the fluid properties is obtained from the experimental results of Yao et al. [15]. All the measurements were conducted under atmospheric pressure conditions and room temperature.

For the boundary conditions, constant velocity block profile was utilized for both continuous and dispersed phase inlets. We set α =1 at the inlet of the dispersed phase and α = 0 at the inlet of the continuous phase. No slip boundary conditions are applied at the walls. Pressure boundary was specified at the outlet of the main channel. Table 2 summarizes the varied boundary conditions for each case investigated. The inlet velocity of the dispersed phase (oil) was kept constant at $u_d = 0{,}0185\,\mathrm{m\,s^{-1}}$ for all 4 cases. The surface tension coefficient between the two fluids is $\sigma = 5{,}37\,\mathrm{mN\,m^{-1}}$. The lengths and dimensions of the square cross-section, the inlet and outlet channels are presented in Figure 2.

TABLE I. Summary of the fluid properties

Fluid	Density ρ - [kg m^{-3}]	Viscosity μ - [mPa s]
Water	995,4	0,89
Oil	689,9	0,53

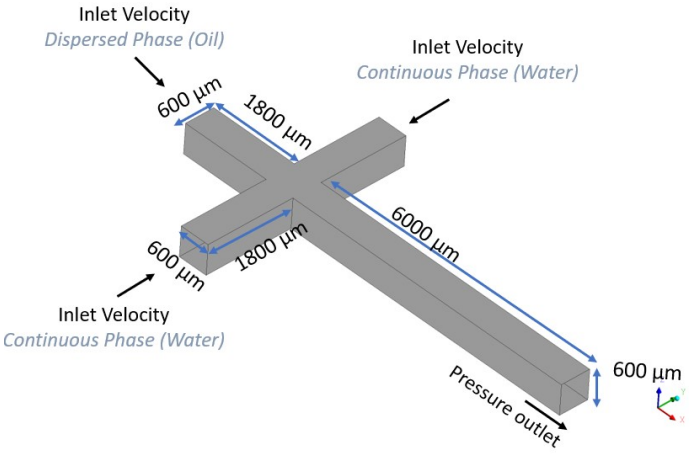

Fig. 2. Model geometry, dimensions and boundary conditions.

III. Results

In order to examine the efficiency of the VOF model, first a validation of the results with the experimental work of Wu et al. [16] is made. Numerical simulations was performed with the same fluid properties and channel dimensions, considered in the mentioned work (for more detailed information about geometry and fluid properties see the work of Wu et al. [16]). In this case water was utilized for the continuous phase and oil for the dispersed. Figure 3 shows the comparison of the droplet formation in the geometries in the two studies. It can be seen that both results have very close time scales regarding the generation of oil (blue) in water (red) droplets. First, the so-called filling stage is observed, where the dispersed phase is injected into the main channel. At some point the growing water-front blocks the flow from the side channels causing the upstream pressure to increase until it reaches a value where the continuous phase begins to squeeze the interface [17]. In the

TABLE II. Simulated cases

Case	u_c - [m s^{-1}]
1	0,0185
2	0,037
3	0,074
4	0,00925

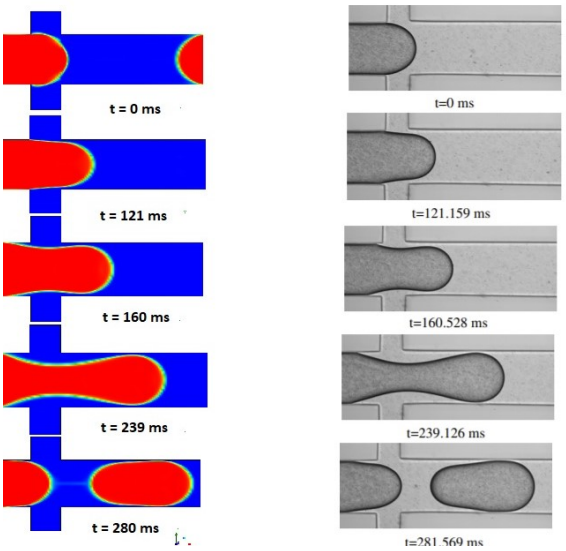

Fig. 3. Visual Comparison between our results (left) and the experiment of Wu et al [16].

second, so called, necking stage the water is still being injected into the droplet at a constant flow rate, while the neck collapses. The collapse accelerates triggering the last pinch-off stage, where the droplet detaching occurs. The three stages described above form, the so-called dripping regime in a flow-focusing microfluidics device [18].

In order to understand better the mechanisms behind droplet formation in flow-focusing generator, four cases with varied continuous phase velocities (at constant dispersed flow rate of $u_d = 0{,}0185\,\mathrm{m\,s^{-1}}$) were carried out. The utilized geometry is shown in Figure 2.

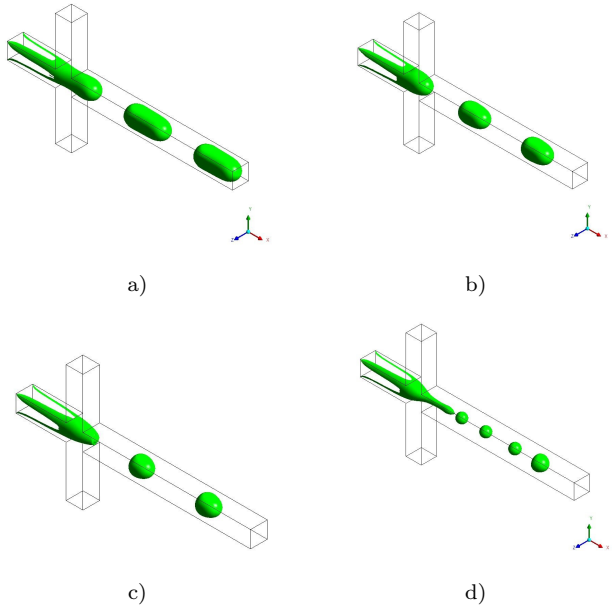

Fig. 4. Isosurfaces of the four simulated cases: a) $u_c = 0{,}009\,25\,\mathrm{m\,s^{-1}}$, b) $u_c = 0{,}0185\,\mathrm{m\,s^{-1}}$, c) $u_c = 0{,}0370\,\mathrm{m\,s^{-1}}$, d) $u_c = 0{,}0740\,\mathrm{m\,s^{-1}}$

The effect of velosity of the continuous phase gets noticeable in Figure 4. Higher continuous phase momentums disrupt the tendency of the surface tension to create few big droplets with less surface energy. Smaller droplets are therefore connected with bigger curvature radii and larger

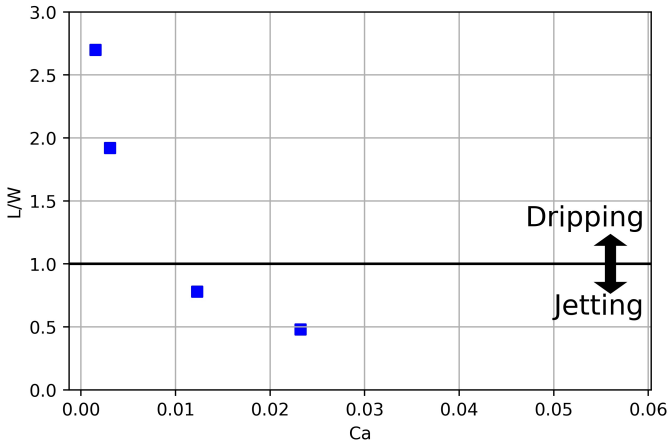

Fig. 5. The nondimensional lenght of the generated droplet as a function of the Ca number.

differences in the pressure jumps between the inside and the outside of a single droplets. It is also clear that smaller droplets creation occurs at higher frequencies. The 'cutting' shear force on the droplets increases at higher velocity ratios, thus making the length of the droplet to decrease. In this, so called jetting regime, a long-suspended column of the disperse fluid flows at the tube as shown in Figures 4d). Naturally, there is a lower limit to the size a particular device can achieve and this is based upon the physical size and individual geometry of that particular device.

One of the critical parameters thoroughly investigated in droplet producing microfluidic devices is the capillary number, described in Equation 5:

$$Ca = \frac{u_c \mu_c}{\sigma} \tag{5}$$

where $_c$ is the dynamic viscosity of the continuous phase. The number identifies the ratio of viscous to interfacial forces. For low capillary numbers, capillary tension dominate leading to the formation of big droplets. Similar to the Reynolds (Re) number, the Ca number can be used to determine a transition-boundary between two flow regimes. One way to do this is to show the geometrical changes in the generated droplets as a function of Ca. Figure 5 shows the non-dimensional length of the droplets (ratio between the lenght of the droplet L and the width of the chanel W) for the 4 cases as a function of the Capillary number. In the Figure it can be seen that the largest changes of the drop size occur up to $Ca \approx 0,01$. The transition between the two main flow regimes - dripping and jetting - occurs at $\frac{L}{W} \approx 1$. There is an indication that for even larger Ca numbers the droplet size does not change significantly.

IV. Conclusion

In this work the droplet generation in a flow-focusing microfluidic device has been investigated. The continuous phase (water) was introduced through the two side channels and the dispersed phase (oil: octane +2,5 % SPAN 80) was entered from the main channel. For all simulations the VOF method was utilized. After a validation of the model was carried out, the investigation of the influence of different velocities of the continuous phase on the droplet formation was simulated. Two flow regimes are formed –

dripping and jetting, which are distinguished by the size of the droplet (for jetting droplets are smaller than the width of the channel). The transition between these regimes is investigated. This is done for a wide range of velocities u_c ($0{,}0740\,\mathrm{m\,s^{-1}} > u_c. > 0{,}009\,25\,\mathrm{m\,s^{-1}}$). There is a critical Ca number, which serves as a transition point between the two described flow regimes (dripping and jetting). For the cases with water as a continuous phase, a critical value of around $Ca \approx 0,01$ is observed. As a whole, the present study shows that the VOF method is a reliable technique for the simulation and prediction of droplet generation in a flow-focusing channels. It will allow the future study of other diverse setups and various fluid combinations.

References

[1] N. Nguyen and S. Wereley, *Fundamentals and Applications of Microfluidics*; Artech House Publishing: Norwood, MA, USA, (2007), 3rd ed. Harlow, England: Addison-Wesley,

[2] E. Grigorov, B. Kirov, M. Marinov and V. Galabov *Review of Microfluidic Methods for Cellular Lysis*, vol. 12, Micromachines 2021, 498

[3] Y. Xu, Z. Zhang, Z. Zhou, X. Han and X. Liu,*Continuous Microfluidic Purification of DNA Using Magnetophoresis*,vol. 11, Micromachines 2020, 187

[4] B.K. Madhusudan, G. Sanket,*Advances in continuous-flow based microfluidic PCR devices—a review*, vol. 2, Eng. Res. Express 2020, 042001

[5] N. Shembekar, C. Chaipan, R. Utharala and C. A. Merten *Droplet-based microfluidics in drug discovery, transcriptomics and high-throughput molecular genetics*, vol. 16, Lab Chip 2016, 1314-1331

[6] T. Thorsen, R. W. Roberts, F. H. Arnold and S. R. Quake *Dynamic Pattern Formation in a Vesicle-Generating Microfluidic Device*, vol. 86, Phys. Rev. Lett. 2001, 4163—4166

[7] W. Zeng and H. Fu *Precise droplet formation in a T-junction micro-droplet generator*, vol. 86, IEEE 8th International Conference on Fluid Power and Mechatronics (FPM) 2019, 1190-1196

[8] S. L. Anna, N. Bontoux and H. A. Stone *Formation of dispersions using "flow focusing" in microchannels*, vol. 82, Appl. Phys. Lett. 2003, 364—366

[9] L. Yobas ,S. Martens, W. L. Ong and N. Ranganathan *High-performance flow-focusing geometry for spontaneous generation of monodispersed droplets*, vol. 6, Lab Chip 2006, 1073 —1079

[10] C. Cramer, P. Fischer and E. J. Windhab *Drop formation in a co-flowing ambient fluid*, vol. 59, Chem. Eng. Sci. 2004, 3045—3058

[11] W. Lan, S. Li, Y. Wang and G. Luo *CFD Simulation of Droplet Formation in Microchannels by a Modified Level Set Method*, vol. 53, Ind. Eng. Chem. Res. 2014, 4913

[12] Y. Li, M. Jain, Y. Ma and Nandakumar *Control of the breakup process of viscous droplets by an external electric field inside a microfluidic device.*, vol. 11, Soft Matter 2015, 3884

[13] A. Gupta, H. S. Matharoo, D. Makkar and R. Kumar *Geometry Effects of Axisymmetric Flow-Focusing Microchannels for Single Cell Encapsulation*, vol. 100,Comput. Fluids 2018, 218

[14] C. Yao, Y. Liu, C. Xu, S. Zhao and G. Chen, *Formation of Liquid-Liquid Slug Flow in a Microfluidic T-junction: Effects of Fluid Properties and Leakage Flow*, vol. 64, AIChE J. 2018, 346

[15] K. Ghaib *The Volume of Fluid Method, a Method for the Simulation of Two-Phase Flow* , Chemie Ingenieur Technik 2018, 316-323

[16] L. Wu, M. Tsutahara, L. S. Kim and M. Ha, *Three-dimensional lattice Boltzmann simulations of droplet formation in a cross-junction microchannel*, vol. 34,Int. J. Multiphase Flow 2008, 852

[17] P.A. Romero and A.R. Abate *Flow focusing geometry generates droplets through a plug and squeeze mechanism*, vol. 12, Lab Chip 2012, 5130-5132

[18] X. Chen, T. Glawdel and N. Cui *Advances in Droplet-Based Microfluidic Technology and Its Applications*, vol. 18, Microfluid Nanofluid 2015, 1341–1353